A Metal-Chelating Lipid for 2D Protein Crystallization *via* Coordination of Surface Histidines

Daniel W. Pack, Guohua Chen, Kevin M. Maloney, Chao-Tsen Chen,[†] and Frances H. Arnold*

Contribution from the Division of Chemistry and Chemical Engineering, 210-41, California Institute of Technology, Pasadena, California 91125

Received November 27, 1996[⊗]

Abstract: Two-dimensional protein crystallization on lipid monolayers is becoming a powerful technique for structure determination as well as materials applications. However, progress has been hindered by the requirement of a unique affinity lipid for each new protein of interest. Metal ion coordination by surface-accessible histidine side chains provides a convenient and general method for targeting of proteins to surfaces. Here we present the synthesis and characterization of a metal-chelating lipid which has been designed to target proteins to Langmuir monolayers and promote their two-dimensional crystallization based on histidine coordination. The lipid utilizes the metal chelator iminodiacetate (IDA) as the hydrophilic headgroup and contains unsaturated, oleyl tails to provide the fluidity necessary for two-dimensional protein crystallization. The lipid is shown to bind copper from the subphase strongly when incorporated in Langmuir monolayers. In addition, it is possible to form copper-containing monolayers by spreading the premetalated lipid on the subphase in the absence of copper. Fluorescence microscopy reveals the binding and crystallization of the protein streptavidin, promoted by the simultaneous coordination of two surface-accessible histidine side chains to the IDA−Cu lipid.

Introduction

Living cells are capable of utilizing their inherently ordered cellular membranes as a template to direct the growth of organized materials. One example is the growth of two-dimensional protein or glycoprotein crystals known as S-layers which form the outermost layer of a wide variety of Gram-positive and Gram-negative bacteria.[1−3] In their natural environments, S-layers function as structure-maintaining elements, protective coats, molecular sieves, and recognition elements. These naturally ordered structures have been employed as molecular filters with a steep exclusion cutoff,[4] patterned immobilization and affinity matrices,[5] biosensors,[6] and patterning masks for nanolithography.[7]

2D protein crystals can also be grown *ex vivo*, on Langmuir monolayers of lipids.[8,9] Crystalline protein arrays have applications in such diverse fields as structural biology and materials science. Perhaps the most obvious application of 2D protein crystals is for structure determination by electron diffraction.[10,11] Recent technological developments have al-lowed near-atomic resolution structures to be obtained from 2D streptavidin crystals grown on biotinylated lipid monolayers.[12] Furthermore, 2D protein crystals may be useful for seeding the epitaxial growth of three-dimensional protein crystals[13,14] and may allow the crystallization of proteins or multiprotein complexes which are difficult to crystallize by other methods.

2D protein crystallization requires the immobilization and orientation of protein at the monolayer surface in high concentration, without loss of mobility.[15] Lateral and rotational mobilities of the bound protein are required to allow its self-organization, formation of the optimum intermolecular contacts, and efficient packing within the crystal. This mobility is supplied largely by the lipid monolayer. Crystallization is generally performed using fluid-phase monolayers, and lipids with unsaturated hydrocarbon tails are employed to provide this fluidity.[16−19]

To date, a significant number of proteins and peptides have been crystallized on Langmuir monolayers.[15] Various classes of interactions have been employed for targeting proteins to the interface. In most cases, specific ligands have been used to promote crystallization of antibodies, enzymes, polypeptide toxins, and other proteins (e.g., streptavidin, annexin VI). In each instance, a unique lipid containing the appropriate affinity ligand was required, and in many cases a novel synthesis of

* To whom correspondence should be addressed. Fax: (818) 568-8743. E-mail: frances@cheme.caltech.edu.
† Current address: Box 768 Havemeyer Hall, Columbia University, New York, NY 10027.
⊗ Abstract published in *Advance ACS Abstracts,* February 15, 1997.

(1) Messner, P.; Sleytr, U. B. *Adv. Microb. Physiol.* **1992**, *33*, 213−275.
(2) Beveridge, T. J. *Curr. Opin. Struct. Biol.* **1994**, *4*, 204−212.
(3) Taylor, K. A.; Deatherage, J. F.; Amos, L. A. *Nature* **1982**, *299*, 840−842.
(4) Sára, M.; Sleytr, U. B. *J. Membr. Sci.* **1987**, *33*, 27−49.
(5) Sára, M.; Küpcü, S.; Weiner, C.; Weigert, S.; Sleytr, U. B. In *Advances in Bacterial Paracrystalline Surface Layers*; Beveridge, T. J., Koval, S. F., Eds.; Plenum Press: New York, 1993; pp 195−204.
(6) Pum, D.; Sára, M.; Sleytr, U. B. In *Immobilized Macromolecules: Application Potential*; Sleytr, U. B., Messner, P., Sára, M., Pum, D., Eds.; Springer-Verlag: London, 1992; pp 141−160.
(7) Douglas, K. In *Biomimetic Materials Chemistry*; Mann, S., Ed.; VCH Publishers, Inc.: New York, 1996; pp 117−142.
(8) Fromherz, P. *Nature* **1971**, *231*, 267−268.
(9) Uzgiris, E. E.; Kornberg, R. D. *Nature* **1983**, *301*, 125−129.
(10) Newman, R. H. *Electron Microsc. Rev.* **1991**, *4*, 197−203.
(11) Jap, B. K.; Zulauf, M.; Scheybani, T.; Hefti, A.; Baumeister, W.; Aebi, U.; Engel, A. *Ultramicroscopy* **1992**, *46*, 45−84.
(12) Avila-Sakar, A. J.; Chiu, W. *Biophys. J.* **1996**, *70*, 57−68.
(13) Edwards, A. M.; Darst, S. A.; Hemming, S. A.; Li, Y.; Kornberg, R. D. *Struct. Biol.* **1994**, *1*, 195−197.
(14) Darst, S. A.; Edwards, A. M. *Curr. Opin. Struct. Biol.* **1995**, *5*, 640−644.
(15) Kornberg, R. D.; Darst, S. A. *Curr. Opin. Struct. Biol.* **1991**, *1*, 642−646.
(16) Ribi, H. O.; Reichard, P.; Kornberg, R. D. *Biochemistry* **1987**, *26*, 7974−7979.
(17) Lebeau, L.; Regnier, E.; Schultz, P.; Wang, J. C.; Mioskowski, C.; Oudet, P. *FEBS Lett.* **1990**, *267*, 38−42.
(18) Lebeau, L.; Oudet, P.; Mioskowski, C. *Helv. Chim. Acta* **1991**, *74*, 1697−1706.
(19) Kubalek, E. W.; Le Grice, S. F. J.; Brown, P. O. *J. Struct. Biol.* **1994**, *113*, 117−123.

this lipid was necessary. For many potentially interesting proteins, however, no convenient affinity ligand is available. Nonspecific electrostatic interactions may be sufficient to induce crystallization when the surface charge on the protein is asymmetric, promoting adsorption with a specific orientation, but this approach is not generally applicable. The difficulty of identifying and obtaining appropriate lipids for targeting and crystallization is certainly a serious limitation to progress in this field.

It has recently been shown that proteins can be targeted to lipid surfaces through coordination of amino acid side chains to lipid-bound metal ions.[20-23] At neutral pH, histidine side chains are primarily responsible for the affinity of metal ions for protein surfaces (e.g., $K_a \approx 10^{3.5}$ M^{-1} for a single histidine interaction with iminodiacetate-chelated Cu^{2+}); at slightly basic pH, other groups such as lysine and the N-terminus can also contribute to metal binding.[24] This interaction should be useful for 2D crystallization studies of proteins displaying surface histidines. In fact, nitrilotriacetate−nickel(II) (NTA−Ni) lipids have been utilized by Kubalek *et al.* for the 2D crystallization of a polyhistidine-tagged HIV-1 reverse transcriptase.[19] Iminodiacetate−copper (IDA−Cu) lipids provide a higher affinity for histidine than NTA−Ni and can therefore effectively target proteins *via* coordination of naturally-occurring surface histidines which lipids containing the NTA-Ni complex cannot.[20] Thus, IDA−Cu lipids can potentially extend this approach to a wide variety of proteins with solvent-accessible histidines, either natural or genetically engineered.

Here we report the synthesis and monolayer characterization of the metal-chelating lipid 1,1′-[[9-[2,3-bis[(Z)-octadec-9-enyloxy]propyl]-3,6,9-trioxanonyl]imino]diacetic acid (DOIDA) which was specifically designed for 2D crystallization. Unsaturated oleyl tails are utilized to provide the required monolayer fluidity. The metal chelator IDA, which strongly binds divalent transition metal ions such as copper ($K_a \approx 10^{10.6}$ M^{-1}),[25] is used as the hydrophilic headgroup. The IDA is attached to the glycerol backbone *via* a triethylene glycol spacer (∼11.5 Å long) which ensures the IDA−Cu complex is displayed in the aqueous subphase and is available for ligand binding. The utility of this lipid for 2D protein crystallization is demonstrated using the tetrameric protein streptavidin, known for its ability to very tightly bind 4 equiv of the small molecule biotin ($K_a \approx 10^{15}$ M^{-1}).[26] Streptavidin has been crystallized previously in two dimensions on Langmuir monolayers of biotin-containing lipids[27] and on monolayers of poly(1-benzyl-L-histidine) *via* nonspecific, electrostatic interactions.[28] Our initial observations of streptavidin crystallization on DOIDA−Cu monolayers using Brewster angle microscopy have been reported previously.[29] In the present work, fluorescence microscopy is used to confirm and further characterize the streptavidin crystallization process.

(20) Shnek, D. R.; Pack, D. W.; Sasaki, D. Y.; Arnold, F. H. *Langmuir* **1994**, *10*, 2382−2388.

(21) Ng, K.; Pack, D. W.; Sasaki, D. Y.; Arnold, F. H. *Langmuir* **1995**, *11*, 4048−4055.

(22) Dietrich, C.; Schmitt, L.; Tampé, R. *Proc. Natl. Acad. Sci. U.S.A.* **1995**, *92*, 9014−9018.

(23) Dietrich, C.; Boscheinen, O.; Scharf, K.-D.; Schmitt, L.; Tampé, R. *Biochemistry* **1996**, *35*, 1100−1105.

(24) Johnson, R. D.; Todd, R. J.; Arnold, F. H. *J. Chromatogr.* **1996**, *725*, 225−235.

(25) Martell, A. E.; Smith, P. M.*Critical Stability Constants*; Plenum Press: New York, 1974; Vol. 6.

(26) Green, N. M. *Adv. Protein Chem.* **1975**, *29*, 85−133.

(27) Darst, S. A.; Ahlers, M.; Meller, P. H.; Kubalek, E. W.; Blankenburg, R.; Ribi, H. O.; Ringsdorf, H.; Kornberg, R. D. *Biophys. J.* **1991**, *59*, 387−396.

(28) Furuno, T.; Sasabe, H. *Biophys. J.* **1993**, *65*, 1714−1717.

(29) Frey, W.; Schief Jr., W. R.; Pack, D. W.; Chen, C.-T.; Chilkoti, A.; Stayton, P.; Vogel, V.; Arnold, F. H. *Proc. Natl. Acad. Sci. U.S.A.* **1996**, *93*, 4937−4941.
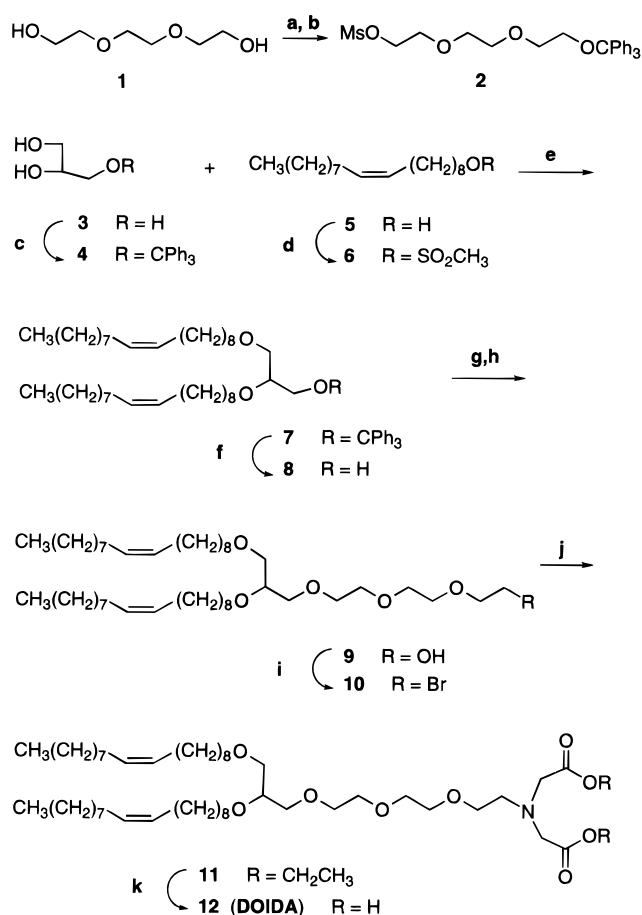

Figure 1. (a) MsCl, CH$_2$Cl$_2$, Et$_3$N, 12 h. (b) Trityl chloride, DMAP, Et$_3$N, CH$_2$Cl$_2$, 12 h, 42%. (c) Trityl chloride, DMAP, Et$_3$N, THF, 12 h, 76%. (d) MsCl, CH$_2$Cl$_2$, Et$_3$N, 12 h, 86%. (e) Powdered KOH, DMSO, 80 °C, 36 h, 33%. (f) TsOH, THF/CH$_3$OH, room temperature, 12 h, 67%. (g) NaH, 1-(methylsulfonyl)-9-(triphenylcarbinyl)-3,6,9-trioxynonane (**2**), THF, reflux, 12 h. (h) TsOH, THF/CH$_3$OH, room temperature, 12 h, 90%. (i) CBr$_4$, PPh$_3$, THF, 0 °C to room temperature, 12 h, 75%. (j) Diethyl iminodiacetate, Et$_3$N, THF, 72 h, 21%. (k) NaOH, THF/MeOH/H$_2$O, reflux, 1 h, 41%.

Results

Lipid Synthesis. Dioleyl lipid **12** (DOIDA) was synthesized as outlined in Figure 1. DOIDA features a glycerol backbone connecting two ether-linked oleyl tails at the 2 and 3 positions and a hydrophilic spacer to the iminodiacetate headgroup on the 1 position. Trityl-protected glycerol **4** and oleyl mesylate **6** were coupled to produce **7**. Deprotection of the trityl group and esterification with 1-(methylsulfonyl)-10-(triphenylcarbinyl)-1,4,7,10-tetraoxadecane (**2**), prepared from triethylene glycol, introduced the triethylene glycol spacer group to the main lipid body **9**. The hydroxyl group of **9** was then substituted with bromine, which was subsequently substituted by diethyl iminodiacetate. Hydrolytic cleavage of the ethyl ester groups of **11** led to the final product DOIDA (**12**).

Langmuir Monolayer Characterization of DOIDA. Surface pressure−molecular area ($\pi-A$) isotherms are sensitive to changes in molecular organization of amphiphiles at the air−buffer interface and can reflect the presence of molecules in the aqueous subphase which are capable of interacting with the monolayer components.[30] Changes in the $\pi-A$ isotherms of the metal-chelating DOIDA have been used to observe Cu^{2+} binding by the IDA headgroups. In order to check for oxidation

(30) Gaines, G. L. *Insoluble Monolayers at Liquid-Gas Interfaces*; Wiley (Interscience): New York, 1966.
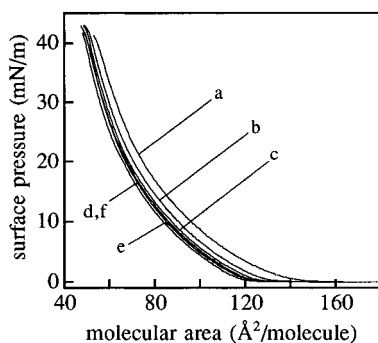
Figure 2. Surface pressure−molecular area isotherms of pure DOIDA lipid in the presence of varying amounts of CuCl$_2$: (a) no divalent metal; (b) 0.20 μM CuCl$_2$; (c) 0.35 μM CuCl$_2$; (d) 0.50 μM CuCl$_2$; (e) 1.0 μM CuCl$_2$; (f) 10 μM CuCl$_2$ on a buffered subphase (20 mM MOPS, 100 mM NaCl, pH 7.5, 25 °C).

of the unsaturated tails, $\pi-A$ isotherms were measured on monolayers under both Ar and ambient atmospheres. No difference in the $\pi-A$ isotherms was observed, and the experiments described herein were performed under ambient atmosphere.

Isotherms of Langmuir monolayers of DOIDA with varying amounts of CuCl$_2$ (0−10 μM) in the buffered subphase are shown in Figure 2. Owing to their unsaturated tails, the DOIDA lipids remain in an expanded phase throughout the compression; no phase transition is observed in the isotherms at any surface pressure or any copper concentration. However, we do observe a decrease in area with increasing copper concentration in the subphase. Adding 10 μM CuCl$_2$ to the subphase results in a decrease in the take-off area from 145 to 120 Å^2/molecule and a similar, yet smaller, decrease in area at all pressures (e.g., from 75 to 66 Å^2/molecule at $\pi = 20$ mN/m).

For many applications, including 2D crystallization of streptavidin, it is necessary to form a metal-containing monolayer in the absence of free Cu^{2+} in the subphase. Thus, monolayers were spread from a premetalated lipid solution; the lipid headgroups were loaded with copper by adding a slight molar excess (less than 10 mol %) of CuCl$_2$ in MeOH to the lipid solution in CHCl$_3$. Isotherms of the premetalated lipids on a metal-free subphase are identical to those of the metal-free lipid spread on a subphase containing 10 μM CuCl$_2$ (data not shown).

2D Protein Crystallization. Because Cu^{2+} in solution was found to inhibit binding and crystallization of streptavidin even under a biotinylated lipid monolayer,[29] the chelating lipids were loaded with Cu^{2+} prior to spreading the monolayers. In each experiment, streptavidin was injected beneath the DOIDA−Cu monolayer at a surface pressure of 3−4 mN/m to final protein concentrations in the aqueous subphase of 20−120 nM. Although the presence of Ar had no effect on $\pi-A$ isotherms of DOIDA, all crystallization experiments with DOIDA−Cu were performed under an inert Ar atmosphere to prevent oxidation of the unsaturated tails during the often long time period (∼4 h) required for crystallization.

Fluorescence micrographs demonstrating the crystallization of rhodamine-labeled streptavidin on a DOIDA−Cu monolayer are shown in Figure 3. In this experiment, the first aggregates began to appear nearly 2 h after protein was injected. The earliest observed aggregates are irregular in shape. At longer times, the aggregates took on a characteristic rectangular shape. The aggregates continued to grow in size over approximately 4 h, maintaining the rectangular shape at all times. Finally, the aggregates became quite large (∼50 × 50 μm^2), covering most of the monolayer area. At this point, the aggregates ceased to

grow, and the monolayer became very stiff as evidenced by its resistance to convection. Protein aggregates of all sizes tend to associate with one another, as groups of aggregates are more common than individual "tiles". Furthermore, the tiles were observed to interlock primarily at the corners or on the flat sides; contacts between corners and flat sides were rare. However, the sharp edges and square corners were maintained even in very dense groupings of large tiles. (It should be noted that the relatively bright background in these images is due to free, out-of-focus protein in solution through which the excitation and emission light must pass, due to the inverted microscope configuration.)

Two control experiments indicate that streptavidin binding by the IDA lipid requires the presence of copper ions. Injection of the soluble metal chelator ethylenediaminetetraacetate (EDTA) into the subphase beneath mature streptavidin crystals caused the protein crystals to disappear within 15−30 min. EDTA can remove Cu^{2+} from the IDA lipid (log $K = 18.7$ compared to log $K = 10.6$ for IDA[25]). In addition, no protein was bound to the interface after injection of the same amount of streptavidin underneath a DOIDA monolayer in the absence of Cu^{2+}.

Crystallization experiments were carried out under both constant surface pressure and constant area conditions. Domain formation and growth proceeded in a similar fashion in both cases. Protein binding could be observed through changes in the surface pressure−molecular area behavior of the monolayer. Typical plots of the changes in surface pressure and molecular area as functions of time are shown in Figure 4. In constant area experiments, surface pressure began to increase immediately after protein injection (Figure 4a). The first aggregates appeared after a pressure increase of 1.8 mN/m. As the tiles grew, the surface pressure continued to increase and reached saturation ($\Delta\pi = 5$ mN/m) at about the same time the tiles stopped growing and the monolayer became stiff. Similar results were obtained in constant surface pressure experiments (Figure 4b). The first aggregates appeared after an area increase ($\Delta A/A$) of 0.20. The area continued to increase as the tiles grew, and the area change reached saturation ($\Delta A/A = 0.45$) as the streptavidin tiles reached their maximum size (∼75 × 75 μm^2).

Polarized fluorescence microscopy was used to investigate the degree of ordering and visualize the relative orientations of the streptavidin domains. In this experiment, two polarizing filters are placed on a slider in the excitation light path with their directions of polarization perpendicular to one another. Fluorophores whose absorption dipoles are aligned with the polarization of the excitation light are selectively excited and are, therefore, observed. Fluorophores whose absorption dipoles are aligned perpendicular to the excitation light do not absorb and do not emit fluorescence. An amorphous phase, in which fluorophores are randomly aligned, will emit fluorescence of equal intensity regardless of the orientation of the polarizing filters. In contrast, a crystalline phase is expected to display a single orientation of fluorophores. Thus, a crystal which appears bright when viewed through a particular polarizer will appear darker when viewed through a perpendicularly oriented polarizer.

Pairs of fluorescence micrographs showing streptavidin domains viewed under perpendicular orientations of the polarizers are shown in Figure 5. These tiles, while appearing to be largely aggregated with one another, retain the characteristic sharp edges and square corners of crystals grown on DOIDA−Cu monolayers. The inverted contrast in each pair of images is readily apparent, suggesting the protein domains are indeed crystalline.[31] Surprisingly, the tiles appear to be oriented with one another within individual aggregates, indicating the tiles
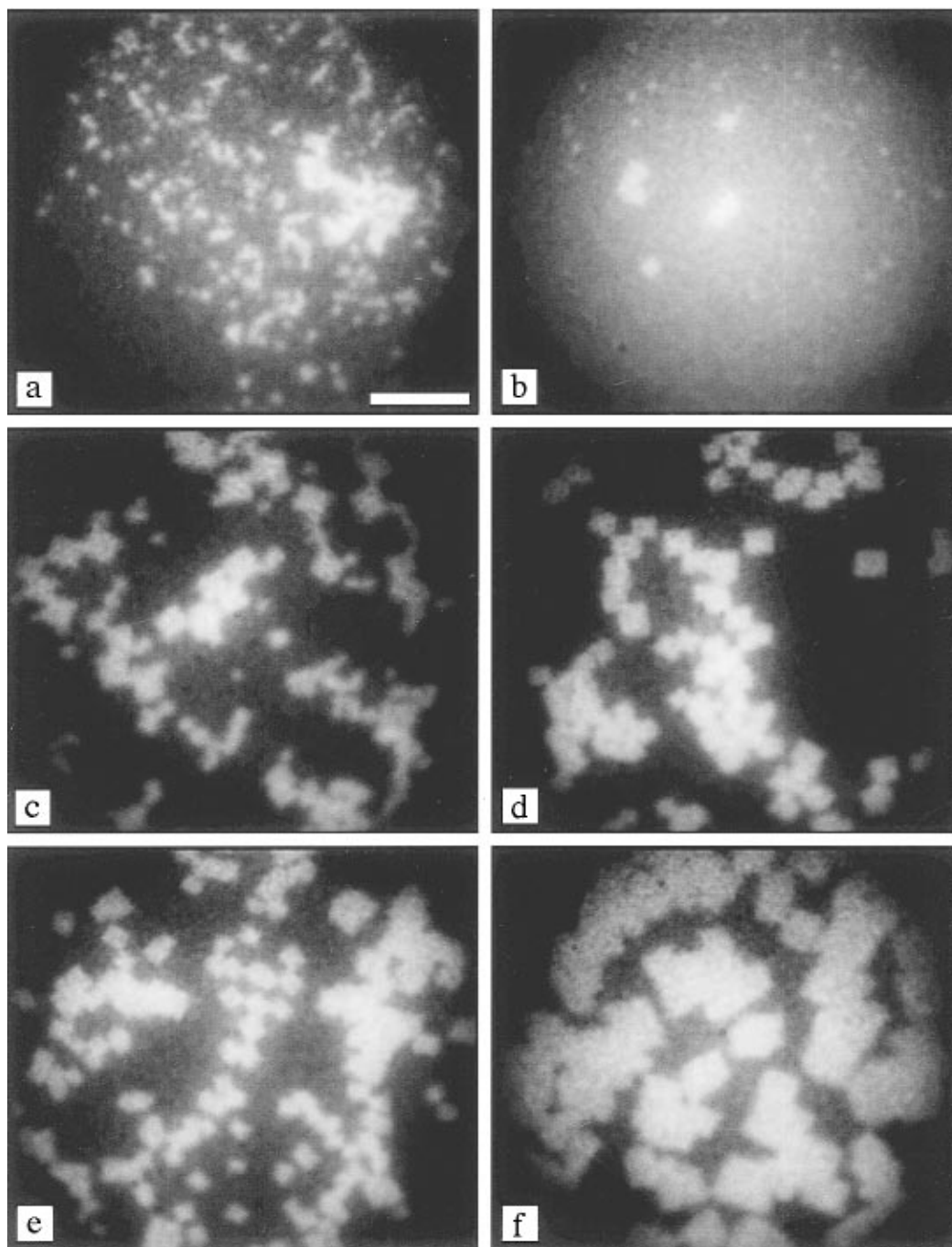
Figure 3. Time sequence of fluorescence micrographs of 2D streptavidin self-assembly beneath a DOIDA−Cu monolayer (3 mN/m) on a buffered subphase (20 mM MOPS, 250 mM NaCl, pH 7.8) at room temperature. The streptavidin concentration is ∼80 nM. Images were taken (a) 115, (b) 125, (c) 150, (d) 190, (e) 200, and (f) 250 min after protein injection. Scale bar = 100 μm.

either arose from a single nucleation site or, more likely, became aligned as they aggregated.
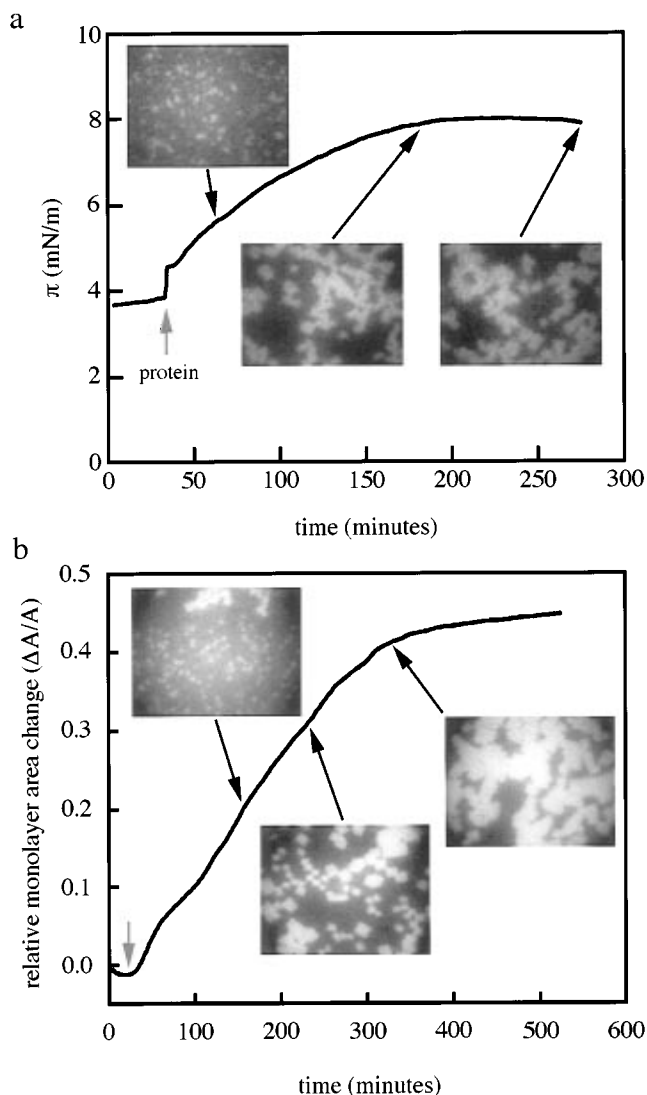
Biotin Disrupts 2D Streptavidin Domains. Mature streptavidin domains grown on DOIDA−Cu monolayers rapidly disappeared upon injection of biotin into the subphase at 4−40-fold molar excess over the total protein concentration. Even when stoichiometric quantities of biotin (4-fold excess) were added, the protein disappeared from the interface within 5 min.

In addition, biotin-loaded streptavidin failed to bind DOIDA−Cu monolayers or an IDA−Cu-derivatized chromatography matrix.[29] These results are rather surprising as biotin is not expected to affect the IDA−Cu−His complex directly, and its binding by streptavidin causes only small perturbations in the protein structure.[32]

A variety of biotinylated molecules spanning a wide range of molecular sizes is capable of disrupting the protein domains. Addition of biotinylated fluorescein (see the Experimental Section), at a 4-fold molar excess over the streptavidin concentration, resulted in disappearance of protein from the interface within 5 min. Injection of a biotinylated lysozyme caused the disappearance of streptavidin from the interface

(31) Polarization fluorescence microscopy of the streptavidin domains requires the protein to be labeled at a unique site. The succinimidyl ester chemistry preferentially labels lysine residues and is therefore expected to label a number of residues on the protein surface. However, the polarized fluorescence results indicate the streptavidin is, in fact, labeled at a unique site. Similar results were obtained previously with fluorescein isothiocyanate-labeled streptavidin (Blankenburg, R.; Meller, P.; Ringsdorf, H; Salesse, C. *Biochemistry* **1989**, *28*, 8214−8221.).

(32) Weber, P. C.; Ohlendorf, D. H.; Wendoloski, J. J.; Salemme, F. R. *Science* **1989**, *243*, 85−88.

Figure 4. Surface pressure (a) and relative monolayer area change (b) of a DOIDA−Cu monolayer on a buffered subphase (20 mM MOPS, 250 mM NaCl, pH 7.8) during 2D streptavidin crystallization. The time of protein injection is indicated by the gray arrows. Fluorescence micrographs at 62, 184, and 278 min in (a) show the crystal growth in relation to the pressure change. Fluorescence micrographs at 150, 220, and 270 min in (b) show the crystal growth in relation to the area change.

within 15 min.[33] Finally, a bisbiotin linker was prepared and loaded into a solution of streptavidin. Each of the biotin binding pockets contained one bisbiotin molecule, and the resulting protein displayed four biotin moieties capable of further binding to apostreptavidin. Addition of bisbiotin streptavidin beneath mature tiles of apostreptavidin disrupted the tiles, and the protein completely disappeared from the interface in approximately 45 min.

Discussion

Metal Chelation by DOIDA at the Air−Buffer Interface.
The relatively large compressibility of the DOIDA monolayers

---

(33) Native, unbiotinylated lysozyme in the same concentration also disrupted streptavidin tiles. However, without biotin the process of crystal disruption was accompanied by a large increase in the surface pressure to >20 mN/m and required more than 45 min. Thus, disruption of streptavidin domains by native lysozyme appears to occur by a different mechanism. Most likely, lysozyme binds the IDA−Cu headgroups outside the streptavidin domains, increasing the surface pressure; lysozyme is known to have significant affinity for immobilized metal ions. The surface pressure increase could be responsible for the disappearance of protein from the interface (Vogel, V.; Schief Jr., W. R.; Frey, W. *Supramol. Sci.,* in press).

indicates the lipid is in a fluid state at all surface pressures. In fact, the shape of the $\pi-A$ curve (Figure 2) is very similar to that of fluid dioleoylphosphocholine monolayers.[34] Chelation of Cu^{2+} by the IDA headgroups results in a condensation of the DOIDA monolayer. However, the lipid remains in the fluid state at all copper concentrations. The fluid state is required for growth of 2D protein crystals.[10,15] The condensation of the DOIDA monolayers is very similar to that observed for analogous IDA lipids with differing hydrophobic tails.[35]

The decrease in monolayer area upon metal binding is most likely due to neutralization of the headgroup charge.[35] Changes in the $\pi-A$ isotherm cease as the $CuCl_2$ concentration is increased above 0.50 μM; $\pi-A$ isotherms obtained for monolayers on 0.50, 1.0, and 10 μM $CuCl_2$ are identical. Thus, it is believed the IDA headgroups are saturated with chelated Cu^{2+} at and above 0.50 μM $CuCl_2$. Given a saturation point between 0.35 and 0.50 μM $CuCl_2$, one can estimate a lower limit on the apparent affinity of Cu^{2+} for the IDA headgroup of $(1.3-1.8) \times 10^8$ M^{-1} at pH 7.5. This association constant is smaller than that of IDA for Cu^{2+} in bulk solution $(4 \times 10^{10}$ $M^{-1})$.[25] The discrepancy in binding affinity is likely a result of steric or electrostatic effects due to the very high local concentration of IDA at the interface.

Lipids which have been premetalated in solution prior to spreading of the monolayer result in $\pi-A$ isotherms identical to the unmetalated lipid spread on subphase containing greater than 0.50 μM $CuCl_2$. Thus, premetalated DOIDA−Cu monolayers are believed to be fully loaded with copper. Kinetic studies of the $\pi-A$ behavior of the monolayers have determined that premetalated IDA lipids retain ∼75% of the Cu^{2+} in the headgroup even after 10 h at the air−buffer interface.[36]

Streptavidin Crystallization via Metal Coordination.
Streptavidin forms two-dimensional domains on Langmuir monolayers of the metal-chelating lipid DOIDA. Several lines of evidence indicate that these domains are crystalline. Firstly, their sharp edges and consistent shape, both during growth in a single experiment and from experiment to experiment, strongly suggest the domains are crystalline. Secondly, the polarized fluorescence microscopy results (Figure 5) support their ordered nature. Recently, Fourier analysis of an electron micrograph of DOIDA−Cu-bound streptavidin aggregates indicates the protein is ordered and has shown lattice parameters identical to those of biotin lipid-bound streptavidin crystals.[37] In addition, a filtered image in negative stain produced a low-resolution projection map of the electron density[37] very similar to the known 2D projection of biotin-bound streptavidin crystals at a comparable resolution.[27,38] Streptavidin is known to bind to IDA−Cu lipids *via* His 87, which is located on the same face of the protein as the entrance to the biotin binding pockets.[29] This fact, in combination with the apparent identity of the DOIDA−Cu- and biotin lipid-bound crystal parameters, suggests the protein is oriented similarly in the two cases, with two biotin binding pockets adjacent to the monolayer and two pockets facing away from the monolayer, exposed to the aqueous subphase.

Crystals could be produced from subphase streptavidin concentrations as low as 20 nM. This concentration appears low, given that only two simultaneous IDA−Cu−His 87 interactions are possible, which could indicate that protein−protein interactions play a significant role in stabilization of
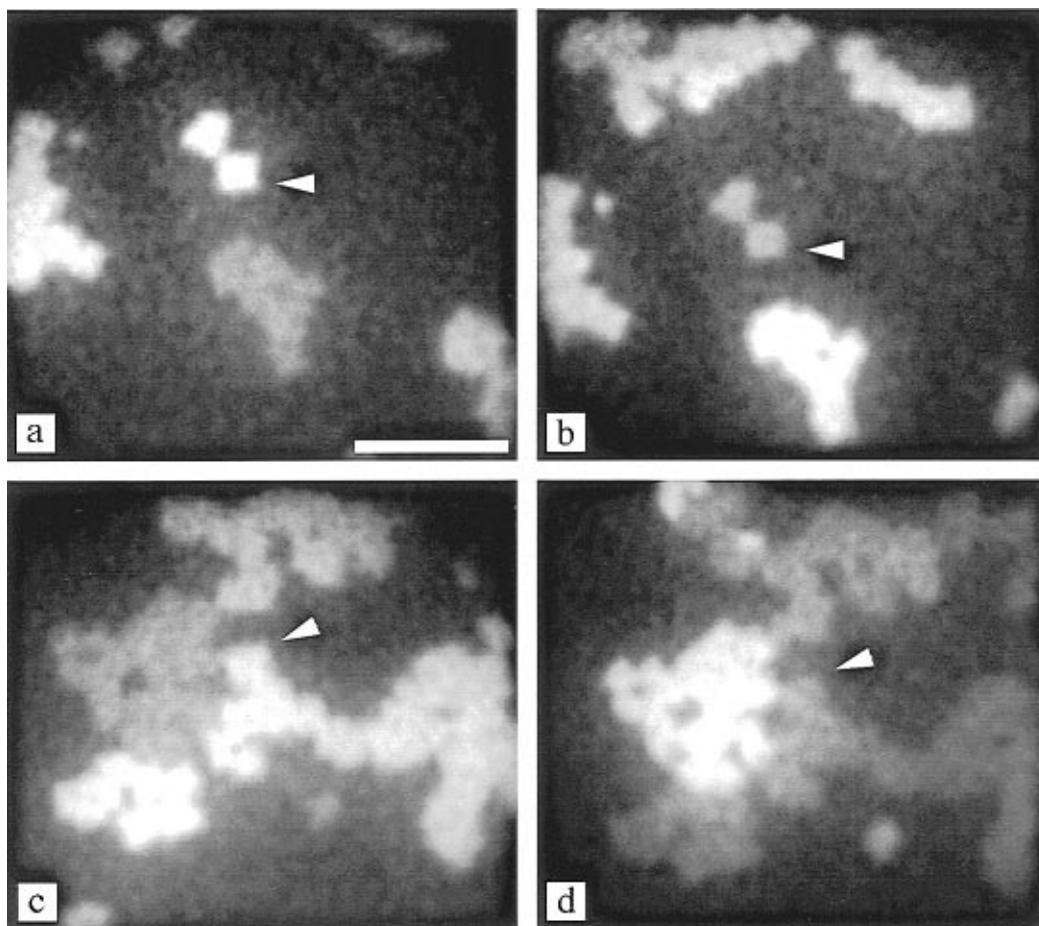
---

(34) Bohorquez, M.; Patterson, L. K. *Langmuir* **1990**, *6*, 1739−1742.
(35) Pack, D. W.; Arnold, F. H. *Chem. Phys. Lipids*, in press.
(36) Pack, D. W. Ph.D. Thesis, California Institute of Technology, 1996.
(37) Chang, W.-H.; Kornberg, R. D. Personal communication.
(38) Ku, A. C.; Darst, S. A.; Robertson, C. R.; Gast, A. P.; Kornberg, R. D. *J. Phys. Chem.* **1993**, *97*, 3013−3016.

Figure 5. Fluorescence micrographs of streptavidin aggregates grown on DOIDA−Cu monolayer on a buffered subphase (20 mM MOPS, 250 mM NaCl, pH 7.8) imaged through polarizing filters. Images on the right and left were taken under perpendicular orientations of the polarizers. White arrowheads indicate equivalent points on the monolayer in each of the pairs of images. Scale bar = 100 μm.

streptavidin binding to the DOIDA−Cu monolayer. In addition, at pH 7.8, other basic groups on the protein such as lysine and the N-terminus can participate in metal coordination and may be contributing to the apparent high affinity of streptavidin for the IDA−Cu lipids.

Streptavidin crystallization on DOIDA−Cu was performed at surface pressures near 3 mN/m. Higher pressures greatly reduced the formation of crystals, and in fact, compression of the monolayer to pressures of 15−20 mN/m destroys the mature crystals.[39] Such low surface pressures in the IDA−Cu lipid monolayers may be required in order to provide sufficient mobility of the lipid and bound protein. However, this seems unlikely as DOIDA−Cu monolayers appear to be in the liquid state at all pressures and are thus expected to be very mobile.

Streptavidin crystallization on biotinylated lipid monolayers is known to depend on the length of the spacer attaching the biotin to the lipid backbone. Very long spacers allow crystallization over a large range of surface pressures, shorter spacers allow crystallization only in the fluid state, and, with no spacer, crystallization occurs only in noncompressed monolayers.[27] The longer spacer is believed to decrease penetration of the protein into the monolayer. Due to differences in (1) the IDA−Cu and biotin lipid structures and (2) the binding site on the protein, it is unclear in which class of spacer length the IDA−Cu lipids should be placed. Nevertheless, the inhibition of crystallization with increasing surface pressure is likely a result of decreasing ability of streptavidin to penetrate the DOIDA−Cu monolayer. A requirement for partial penetration of the protein into the lipid bilayer also explains the increase in surface pressure or

monolayer area observed during crystallization (Figure 4). We might expect crystallization on IDA−Cu lipid monolayers to be more sensitive to surface pressure than that on biotin lipid monolayers due to the vastly larger affinity of streptavidin for the biotin lipids. This larger binding energy will allow the protein to remain attached to the lipids at higher surface pressures where steric interactions with the monolayer make adsorption less favorable. In fact, streptavidin crystals grown on biotin lipid may be compressed to surface pressures as high as 32 mN/m with no effect on the crystal morphology.[39]

Biotin Binding Affects Metal Binding to Streptavidin. The ability to decorate the crystal surface by binding additional biotinylated molecules to the exposed pockets is desirable for a variety of applications.[40−42] However, addition of biotin, or biotinylated molecules spanning a wide range of sizes, to the subphase below mature streptavidin crystals caused the protein to disappear from the monolayer. The fluorescein−biotin compound disrupted DOIDA−Cu-bound streptavidin crystals as quickly as did free biotin (within 5 min). Lysozyme (MW 14 300) is small enough (∼45 × 30 × 30 Å^3) to access both biotin binding pockets simultaneously (given ∼3600 Å^2 per streptavidin[27]) and disrupted the mature streptavidin crystals in 15 min. Similarly, bisbiotin-containing streptavidin disrupted mature apostreptavidin crystals within 45 min of its injection into the subphase. Loading streptavidin with biotin also

(39) Vogel, V.; Schief Jr., W. R.; Frey, W. *Supramol. Sci.*, in press.

(40) Ahlers, M.; Blankenburg, R.; Grainger, D. W.; Meller, P.; Ringsdorf, H.; Salesse, C. *Thin Solid Films* **1989**, *180*, 93−99.
(41) Herron, J. N.; Müller, W.; Paudler, M.; Riegler, H.; Ringsdorf, H.; Suci, P. A. *Langmuir* **1992**, *8*, 1413−1416.
(42) Samuelson, L. A.; Miller, P.; Galotti, D. M.; Marx, K. A.; Kumar, J.; Tripathy, S. K.; Kaplan, D. L. *Langmuir* **1992**, *8*, 604−608.

A Metal-Chelating Lipid for 2D Protein Crystallization

J. Am. Chem. Soc., Vol. 119, No. 10, 1997 2485

eliminates the strong affinity exhibited by apostreptavidin for copper−IDA in metal affinity chromatography.[29]

These effects may reflect biotin-induced structural changes in streptavidin.[32] Alternatively, biotin binding may disrupt the IDA−Cu-grown crystals by disturbing protein−protein contacts. In fact, binding of biotin to two streptavidin binding pockets on biotin−lipid monolayers affects the protein−protein contacts, resulting in asymmetric crystal growth.[38] However, streptavidin crystallizes on biotin−lipid monolayers, and the two empty biotin sites of these crystals can be loaded with biotin or biotin derivatives in limited quantities without affecting those 2D crystals.[40] Thus, biotin-induced structural changes do not affect the ability of the protein to crystallize in 2D. The effects of biotin on metal ion binding are clearly not fully understood at this time.

Conclusions

Metal ion coordination by surface-accessible histidines, either genetically engineered or naturally occurring, can provide a general method for targeting of proteins to metal-chelating lipid membranes. The ability to immobilize protein on a mobile lipid monolayer is the first step toward 2D protein crystallization. In the present study, coordination of two histidines to DOIDA−Cu monolayers leads to 2D crystallization of streptavidin. The metal-chelating DOIDA−Cu lipid provides the necessary targeting and mobility to promote 2D protein crystallization. Thus, this lipid has the potential to greatly accelerate the investigation of proteins for 2D crystallization and should facilitate the exploration of organized protein arrays as functional materials.

Experimental Section

General Methods. All reactions were performed in oven-dried (160 °C) glassware under positive Ar atmosphere. ^{1}H NMR spectra were recorded on a QE 300 spectrometer and referenced to tetramethylsilane (TMS) at 0.00 ppm in chloroform-d (CDCl$_3$). ^{13}C NMR spectra were recorded on a QE 300 spectrometer operating at 75 MHz and referenced to 77.0 ppm in chloroform-d. Infrared spectra were recorded on a Perkin-Elmer 1600 Series FTIR spectrometer. Mass spectra were obtained from the Center of Biomedical and Bio-organic Mass Spectrometry of Washington University, and from the University of California at Riverside mass spectrometry facility. Chemical analyses were performed by Desert Analytics (Tucson, AZ). Melting points were determined on a Laboratory Devices Mel-Temp II. All flash column chromatography was performed with Merck grade 60 silica gel. Reactions were monitored as a function of time by TLC using J. T. Baker plastic silica gel plates (JT7024-2) with a 40 μm particle size and adsorbent thickness of 250 μm, purchased from VWR Scientific (Chicago).

Materials. Chemical reagents and starting materials were purchased from Aldrich Chemical Co. unless otherwise noted. Tetrahydrofuran was distilled from sodium−benzophenone ketyl. Dichloromethane was distilled from CaH$_2$. DMSO was dried over 3 Å molecular sieves. Methanesulfonyl chloride, triethylamine (Et$_3$N), and diethyliminodiacetate (Kodak) were dried and distilled prior to use. Fluorescein biotin [5-[N-[5-[N-[6-(biotinoylamino)hexanoyl]amino]pentyl]thioureidyl]-fluorescein], 5-(and 6)-carboxytetramethylrhodamine succinimidyl ester (RSE), and succinimidyl 6-biotinamidohexanoate (biotin-SE) were obtained from Molecular Probes, Inc. (Eugene, OR). Native streptavidin was obtained from Boehringer-Mannheim as a lyophilized powder. Chloroform, methanol, and ethanol (all ACS HPLC grade), hexane (99+%), and CuCl$_2$ (99.999%) were obtained from Aldrich (Milwaukee, WI). 3-(N-Morpholino)propanesulfonic acid (MOPS) was obtained from Sigma (St. Louis, MO). All other reagents were used as received without further purification.

1-(Methylsulfonyl)-10-(triphenylcarbinyl)-1,4,7,10-tetraoxadecane (2). Triethylene glycol (**1**) (10.0 g, 66.6 mmol), trityl chloride (14.8 g, 53.1 mmol), and DMAP (320 mg, 2.62 mmol) were dissolved in CH$_2$Cl$_2$ (100 mL) in a 250 mL round-bottom flask. Et$_3$N (18.0 mL,

129 mmol) was added, and the resultant mixture was vigorously stirred at room temperature overnight. CH$_2$Cl$_2$ (70 mL) and water (100 mL) were then added to the flask. The reaction mixture was transferred to a separatory funnel, the solution was shaken, the layers were separated, and the organic layer was collected. The aqueous layer was then further extracted with CH$_2$Cl$_2$ (100 mL). The combined organic layers were washed sequentially with 10% NaHCO$_3$ (70 mL × 2) and brine (100 mL), and dried over MgSO$_4$. Solvent was then removed on a rotovap to yield a yellow viscous oil, which was used directly in the next step without further purification.

The oil obtained from the previous step and Et$_3$N (7.4 mL, 53.1 mmol) were dissolved in CH$_2$Cl$_2$ (60 mL) and were cooled to 0 °C. To this solution was slowly added MsCl (4.1 mL, 53.1 mmol). The reaction mixture was then allowed to warm to room temperature and stirred vigorously overnight. Water (50 mL) and CH$_2$Cl$_2$ (30 mL) were added to the solution, and the mixture was transferred to a separatory funnel. The mixture was shaken, the layers were separated, and the organic layer was collected. The aqueous layer was further extracted with CH$_2$Cl$_2$ (50 mL × 2). The combined organic layers were then washed with 10% NaHCO$_3$ (50 mL) and brine (50 mL), and dried over MgSO$_4$. Solvent was then removed on a rotovap to yield a yellow oil. The oily residue was chromatographed, eluting with EtOAc/hexanes (50:50, R_f = 0.30) to give 13.2 g of a white solid (42% yield): mp 89.0−90.5 °C; ^{1}H NMR (CDCl$_3$) δ 2.94 (s, 3H), 3.23 (t, J = 4.4 Hz, 2H), 3.66 (m, 6H), 3.78 (t, J = 4.4 Hz, 2H), 4.36 (t, J = 4.4 Hz, 2H), 7.27 (m, 9H), 7.45 (m, 6H); ^{13}C{^{1}H} NMR (CDCl$_3$) δ 37.59, 63.26, 69.07, 69.25, 70.69, 70.73, 86.54, 126.97, 127.77, 128.66, 143.99; IR (neat) v 3015.2, 2932.4, 2870.0, 1595.9, 1489.6, 1448.0, 1351.8, 1205.3, 1174.5, 1148.2, 1079.5, 1012.4, 970.5, 917.9, 798.3, 775.2, 763.1, 748.4, 707.5, 650.1, 632.3, 528.4 cm^{-1}. Anal. Calcd for C$_{26}$H$_{30}$O$_6$S: C, 66.36; H, 6.43. Found: C, 66.13; H, 6.22.

1-(Triphenylcarbinyl)glycerol (4). Glycerol (20.0 g, 217 mmol), trityl chloride (15.0 g, 53.8 mmol), and DMAP (150 mg, 1.23 mmol) were placed in a 250 mL round-bottom flask containing 40 mL of dry THF. To this heterogeneous mixture was added Et$_3$N (9 mL, 64.63 mmol), and the resultant mixture was vigorously stirred at room temperature overnight. EtOAc (70 mL) and water (50 mL) were then added to the flask. The reaction mixture was transferred to a separatory funnel, the solution was shaken, the layers were separated, and the organic layer was collected. The aqueous layer was then further extracted with EtOAc (50 mL × 2). The combined organic layers were washed sequentially with 10% NaHCO$_3$ and brine, and dried over Na$_2$SO$_4$. Solvent was then removed on a rotovap to yield a yellow oil which was recrystallized with a benzene/hexanes mixture to give 13.6 g of a white solid (76% yield): mp 103−107 °C; ^{1}H NMR (CDCl$_3$) δ 1.97 (t, J = 3.7 Hz, 1H), 2.49 (d, J = 3.9 Hz, 1H), 3.24 (m, 2H), 3.63 (m, 2H), 3.87 (m, 1H), 7.0−7.5 (m, 15H); ^{13}C{^{1}H} NMR (CDCl$_3$) δ 64.45, 70.18, 71.04, 86.59, 126.98, 127.78, 128.64, 143.80; IR (neat) v 3020.2, 2933.0, 1498.8, 1477.8, 1203.2, 1148.8, 764.5, 706.0, 632.0, 494.7 cm^{-1}. Anal. Calcd for C$_{22}$H$_{22}$O$_3$: C, 79.00; H, 6.64. Found: C, 78.88; H, 6.52.

1-[(Methylsulfonyl)oxy]-(Z)-octadec-9-ene (6). Oleyl alcohol **5** (85% purity, 111 g, 0.351 mol) and Et$_3$N (73.5 mL, 0.527 mol) were dissolved in CH$_2$Cl$_2$ (1.2 L) and cooled to 0 °C. To this solution was slowly added MsCl (32.6 mL, 0.422 mol). A white precipitate was observed during the addition. The reaction mixture was then slowly allowed to warm to room temperature and stirred vigorously overnight. Water (500 mL) was added to the solution, and the mixture was transferred to a separatory funnel. The mixture was shaken, the layers were separated, and the organic layer was collected. The aqueous layer was further extracted with CH$_2$Cl$_2$ (500 mL × 2). The combined organic layers were then washed with 1 N HCl (500 mL), 10% NaHCO$_3$ (500 mL) and brine, and dried over Na$_2$SO$_4$. The solution was concentrated *in vacuo* to give a brown oil, which was dissolved in 1 L of mixed solvent of 80% ethyl acetate and 20% hexane. The solution was stored at −5 °C overnight. The solid formed was filtered off. Concentration of the filtrate yielded 105 g (86%) of 1-[(methylsulfonyl)-oxy]-(Z)-9-octadecene as a colorless oil: ^{1}H NMR (CDCl$_3$) δ 0.88 (t, J = 6 Hz, 3H), 1.27 (br s, 12H), 1.30 (br s, 10H), 1.75 (d, J = 7 Hz, 2H), 2.01 (d, J = 3 Hz, 4H), 3.01 (s, 3H), 4.22 (t, J = 6.6 Hz, 2H), 5.33−5.37 (m, 2H); ^{13}C{^{1}H} NMR (CDCl$_3$) δ 13.96, 22.53, 25.26, 27.04, 28.87, 28.97, 29.18, 29.38, 29.87, 31.76, 37.074, 70.08, 129.53,

129.80; IR (neat) v 3000, 2922, 2853, 1465, 1356, 1177, 833, 724 cm^{-1}; LRFAB (EI$^+$) m/z (relative intensity) 364 [(M + NH$_4$)$^+$, 100], 317 (40), 243 (73); HRFAB calcd for C$_{19}$H$_{42}$NO$_3$S [(M + NH$_4$)$^+$] m/z 364.2885, found 364.2877.

1-[(Triphenylcarbinyl)oxy]-2,3-bis[(Z)-octadec-9-enyloxy)pro-pane (7). Tritylglycerol **4** (8.00 g, 23.09 mmol), dissolved in THF (40 mL), was added to a suspension of powdered KOH (3.3 g, 58.93 mmol) in dry DMSO (100 mL). The mixture was heated to 80 °C and maintained at this temperature for 4 h. Oleyl mesylate **6** (19.2 g, 55.42 mmol) dissolved in 30 mL of THF was added to the reaction mixture at 80 °C *via* a syringe. The mixture became gel-like at first and was heated at 80 °C for 36 h. The reaction was cooled to room temperature, and then EtOAc (150 mL) and H$_2$O (150 mL) were added to the mixture, the mixture was shaken, and the layers were separated. The aqueous layer was extracted with EtOAc (100 mL × 2). The combined organics were washed with water (150 mL) and saturated NaCl (150 mL), and dried over Na$_2$SO$_4$. The solution was concentrated *in vacuo*, and the oily residue was chromatographed, eluting with Et$_2$O/hexanes (5:95, $R_f = 0.30$) to obtain 6.6 g of a colorless oil (33% yield): ^{1}H NMR (CDCl$_3$) δ 0.88 (t, $J = 6$ Hz, 6H), 1.27 (br s, 44H), 1.50−1.65 (m, 4H), 1.90−2.05 (m, 8H), 3.17 (br s, 2H), 3.40 (t, $J = 6.6$ Hz, 2H), 3.52−3.60 (m, 5H), 5.33−5.50 (m, 4H), 7.18−7.80 (m, 15H), 7.46 (d, $J = 7.2$ Hz); ^{13}C{^{1}H} NMR (CDCl$_3$) δ 14.10, 21.01, 22.57, 22.68, 25.90, 27.20, 28.59, 28.84, 28.99, 29.21, 29.31, 29.40, 29.51, 29.73, 29.75, 31.90, 32.59, 64.65, 76.58, 129.77, 129.96, 130.20; IR (neat) v 2926, 2854, 2361, 2249, 1723, 1448, 1377, 1219, 1091, 908, 734, 706, 649, 632 cm^{-1}; LRFAB (EI$^+$) m/z (relative intensity) 857.7 [(M + Na)$^+$, 40], 641.5 (25.0), 621.6 (100), 591.5 (5.0); HRFAB calcd for C$_{58}$H$_{90}$O$_3$-Na [(M + Na)$^+$] m/z 857.6787, found 857.6769.

2,3-Bis[(Z)-octadec-9-enyloxy]propanol (8). Compound **7** (6.50 g, 7.50 mmol) and TsOH·H$_2$O (220 mg, 2.4 mmol) were placed in a mixture of THF (40 mL)/MeOH (40 mL) and stirred overnight at room temperature. Et$_3$N (0.3 mL, 2.3 mmol) was added to consume excess TsOH·H$_2$O, and the reaction solution was concentrated on a rotovap to yield an oil which was purified by flash chromatography, eluting with 75% CH$_2$Cl$_2$/hexane (75:25, $R_f = 0.30$) to give 2.96 g of the desired product (67% yield): ^{1}H NMR (CDCl$_3$) δ 0.86 (t, $J = 6$ Hz, 6H), 1.25 (br s, 24H), 1.27 (br s, 20H), 1.42−1.75 (m, 4H), 1.85−2.25 (m, 9H), 3.40−3.75 (m, 9H), 5.20−5.40 (m, 4H); ^{13}C{^{1}H} NMR (CDCl$_3$) δ 14.11, 22.68, 26.09, 27.20, 29.26, 29.32, 29.51, 29.60, 29.76, 30.06, 31.90, 63.05, 70.37, 70.86, 71.82, 78.23, 129.80, 129.93; IR (neat) v 3300, 3030, 2920, 2854, 1735, 1460, 1380, 1205, 1160, 1070, 720, 450 cm^{-1}; HRFAB calcd for C$_{39}$H$_{77}$O$_3$ [(M + H)$^+$] m/z 593.5872, found 593.5871.

9-[2,3-Bis[(Z)-octadecen-9-yloxy]propyl]-3,6,9-trioxanonanol (9). To a suspension of NaH (60% mineral oil dispersion, 1.68 g, 42.1 mmol) in 60 mL of THF was added compound **8** (5.00 g, 8.44 mmol) dissolved in 60 mL of THF. The resultant suspension was stirred for 2 h at room temperature. 1-(Methylsulfonyl)-10-(triphenylcarbinyl)-1,4,7,10-tetraoxadecane (**2**) (5.95 g, 12.65 mmol) was added to the suspension as a solid, and the reaction mixture was brought to reflux overnight. The reaction mixture was then cooled to room temperature, and water was added. The heterogeneous solution was stirred for a few minutes before being transferred to a separatory funnel. EtOAc (200 mL) was added, the mixture was shaken, the layers were separated, and the organic layer was collected. The aqueous layer was further extracted with EtOAc (200 mL × 2). The combined organic layers were washed with brine and dried over Na$_2$SO$_4$. The filtrate was concentrated on a rotovap to yield a blond residue, which was taken up in THF (50 mL)/MeOH (50 mL). TsOH·H$_2$O (400 mg, 43.5 mmol) was then added to the reaction mixture, which was stirred overnight at room temperature. Et$_3$N (0.40 mL) was added to consume excess TsOH·H$_2$O. The solution was then concentrated *in vacuo* to yield a yellow residue. Flash column chromatography of the residue eluting with EtOAc/hexanes (75:25, $R_f = 0.28$) furnished 5.50 g (90% yield) of the desired compound as a colorless oil: ^{1}H NMR (CDCl$_3$) δ 0.88 (t, $J = 6$ Hz, 6H), 1.28 (br s, 44H), 1.50 (br s, 4H), 1.90−2.20 (m, 9H), 3.46−3.75 (m, 21 H), 5.30−5.40 (m, 4H); ^{13}C {^{1}H} NMR (CDCl$_3$) δ 14.03, 22.60, 25.99, 27.12, 29.18, 29.24, 29.43, 29.50, 29.68, 31.83, 32.52, 61.60, 69.94, 70.26, 70.52, 71.48, 72.51, 129.73, 129.81; IR (neat) v 3400, 2924, 2854, 1737, 1412, 1349, 1196, 1127, 740, 501

cm^{-1}; HRMS (FAB) calcd for C$_{45}$H$_{89}$O$_6$ [(M + H)$^+$] m/z 725.6659, found 725.6641.

9-[2,3-Bis[(Z)-octadec-9-enyloxy]propyl]-1-bromo-3,6,9-triox-anonane (10). Compound **9** (1.64 g, 2.17 mmol) was dissolved in THF (15 mL) and cooled to 0 °C. To the solution were added CBr$_4$ (1.44 g, 4.33 mmol) and PPh$_3$ (1.14 g, 4.33 mmol) as solids. The resultant mixture was stirred at 5 °C for 1 h and then stirred at room temperature overnight. The solution turned yellow, and a white precipitate was also observed within 1/2 h after the complete addition of the reagents. The solid was removed by filtration and washed with cold CH$_2$Cl$_2$. The filtrate was then concentrated *in vacuo* to yield a bright yellow oil. Flash column chromatography of the oil eluting with EtOAc/hexanes (25:75, $R_f = 0.26$) furnished 1.34 g (75% yield) of the desired compound as a colorless oil: ^{1}H NMR (CDCl$_3$) δ 0.88 (t, $J = 6$ Hz, 6H), 1.28 (br s, 44H), 1.50−1.65 (m, 4H), 1.85−2.15 (m, 8H), 3.35−3.70 (m, 19 H), 3.81 (t, $J = 6.3$ Hz, 2H), 5.25−5.45 (m, 4H); ^{13}C{^{1}H} NMR (CDCl$_3$) δ 14.10, 22.66, 26.07, 27.18, 29.24, 29.29, 29.48, 29.62, 29.74, 30.25, 31.88, 32.58, 70.04, 70.55, 70.59, 70.69, 71.19, 71.53, 129.82, 129.89; IR (neat) v 2922, 2853, 1738, 1412, 1352, 1201, 1134, 737, 532 cm^{-1}; HRMS (FAB) calcd for C$_{45}$H$_{88}$O$_5$Br [(M + H)$^+$] m/z 787.5815, found 787.5796.

Diethyl 1,1′-[N-[9-[2,3-bis[(Z)-octadec-9-enyloxy]propyl]-3,6,9-trioxanonyl]imino]diacetate (11). Compound **10** (1g, 1.22 mmol), diethyl iminodiacetate (DEIDA) (0.916 g, 9.64 mmol) and Et$_3$N (0.675 mL, 9.64 mmol), were dissolved in dry CH$_3$CN (16 mL)/THF (3 mL), and the reaction mixture was brought to reflux and maintained at this temperature for three days. The reaction was then cooled to room temperature. Excess solvent was removed on a rotovap to yield an oil, which was dissolved in EtOAc (100 mL). The solution was then washed with 1 N HCl (50 mL), H$_2$O (50 mL), and brine (50 mL) and dried over Na$_2$SO$_4$. The solvent was removed on a rotovap. The yellow oil residue was subjected to flash column chromatography eluting with Et$_2$O/hexane (80:20, $R_f = 0.30$) to give 225 mg of the desired product (21% yield): ^{1}H NMR (CDCl$_3$) δ 0.88 (t, $J = 6$ Hz, 6H), 1.27 (br s, 50H), 1.45−1.60 (m, 4H), 1.95−2.10 (m, 8H), 2.97 (t, $J = 7.2$ Hz, 2H), 3.35−3.75 (m, 23 H), 4.16 (q, $J = 7.2$ Hz, 4H), 5.25−5.45 (m, 4H); ^{13}C{^{1}H} NMR (CDCl$_3$) δ 14.04, 14.17, 22.61, 26.02, 27.13, 29.20, 29.24, 29.43, 29.56, 29.69, 31.83, 53.60, 55.64, 60.45, 69.99, 70.03, 70.28, 70.44, 70.56, 71.47, 129.75, 129.83, 170.98; IR (neat) v 3849, 3745, 2923, 2853, 1738, 1208, 1153, 501 cm^{-1}; HRMS (FAB) calcd for C$_{53}$H$_{102}$NO$_9$ [(M + H)$^+$] m/z 896.7554, found 896.7556.

1,1′-[[9-[2,3-Bis[(Z)-octadec-9-enyloxy]propyl]-3,6,9-trioxanonyl]-imino]diacetic Acid (12, DOIDA). Compound **11** (452 mg, 0.488 mmol) and powdered NaOH (195 mg, 4.88 mmol) were placed in a round-bottom flask charged with a reflux condenser. THF (7 mL), MeOH (7 mL), and H$_2$O (2 mL) were added to the flask, and the mixture was then brought to reflux for 1 h. The reaction was cooled to room temperature and acidified to pH ~1 with concentrated HCl. The solvent was removed *in vacuo*. Flash column chromatography of the yellow oil residue eluting with CHCl$_3$/MeOH/H$_2$O (70:25:5, $R_f = 0.3$) gave 168 mg (0.2 mmol, 41% yield) of the desired product: ^{1}H NMR (CDCl$_3$) δ 0.88 (t, $J = 6$ Hz, 6H), 1.28 (br s, 44H), 1.50−1.65 (m, 4H), 1.90−2.10 (m, 8H), 3.25−4.10 (m, 25 H), 5.25−5.45 (m, 4H), 9.48 (br s, 2H); ^{13}C{^{1}H} NMR (CDCl$_3$) δ 14.16, 22.72, 26.19, 27.27, 29.09, 29.37, 29.58, 29.81, 30.03, 30.20, 31.95, 32.67, 53.74, 70.42, 70.64, 70.78, 70.91, 71.01, 71.08, 71.21, 71.45, 71.55, 71.72, 76.83, 77.26, 77.30, 77.81, 77.93, 129.86, 129.83, 130.30, 130.38, 177.80; IR (neat) v 2970, 2361, 2335, 1738, 1366, 1216, 1207, 1150, 772, 639, 510 cm^{-1}; LRFAB (EI$^+$) m/z (relative intensity) 878.5 [(M + K)$^+$, 15], 448.2 (10.0), 386.2 (100); HRMS (FAB) calcd for C$_{49}$H$_{94}$-NO$_9$ [(M + H)$^+$] m/z 840.6928, found 840.6950.

Streptavidin Crystallization. Lipid solutions were prepared in chloroform. The IDA lipids were premetalated by adding an aliquot of concentrated CuCl$_2$ in methanol to the lipid solutions. Excess Cu^{2+} in the lipid solution is no more than 10%. The monolayer subphase was buffered with 20 mM MOPS and 250 mM NaCl, pH 7.8. The buffer, prepared with Milli-Q water (Milli-Q UV Plus, Millipore, Bedford, MA), was shaken with chloroform to remove organic impurities and, subsequently, shaken with hexane to remove traces of chloroform. Streptavidin concentrations were determined by UV−vis absorption spectroscopy at 280 nm using an extinction coefficient of 136 000 M^{-1} cm^{-1}.

Crystallization was performed under two sets of conditions: constant pressure and constant area. Constant pressure experiments were performed in a computer-controlled Langmuir trough (KSV Instruments, Helsinki) with a surface area of 75×230 mm^2. The entire film balance was placed inside a Plexiglas box, and the atmosphere was purged with Ar. The surface pressure was measured by the Wilhelmy plate method using plates cut from filter paper (Whatman No. 1). The plate was rinsed thoroughly with chloroform and calibrated with stearic acid prior to use. Monolayers were compressed at a constant rate of 3 Å^2/(molecule·min). A 15 min waiting period prior to compression allowed for solvent evaporation. Once the desired surface pressure (3 mN/m) was attained, the instrument was switched to constant pressure mode, and the monolayer was allowed to equilibrate for 15−30 min. The desired amount of protein, dissolved in the above buffer, was injected into the subphase either behind the barrier or through the monolayer and allowed to mix by diffusion. Changes in surface area were recorded as a function of time. After each experiment, the trough was thoroughly cleaned with detergent (RBS 35), Milli-Q purified water, and chloroform. All measurements were performed at room temperature, 20−27 °C.

Constant area experiments were performed in a Petri dish hydrophobized with octadecyltrichlorosilane. Holes cut in the lid of the Petri dish allowed access of the Wilhelmy plate and entrance of Ar. Surface pressure was again measured using Wilhelmy plates cut from filter paper. Monolayers were spread dropwise until the desired surface pressure (3 mN/m) was attained. Time was allowed between drops for stabilization of the surface pressure. Thirty to forty-five minutes after spreading, a concentrated streptavidin solution was injected into the 15 mL subphase through the monolayer. Surface pressure was measured as a function of time.

Labeling of Proteins. Streptavidin was labeled with 5-(and 6)-carboxytetramethylrhodamine succinimidyl ester (RSE) following the standard procedure[43] with a slight modification as described.[36] Briefly, 10 mM RSE in dry DMF was added dropwise, with stirring, to a solution of 20−100 µM streptavidin (in 0.1 M NaHCO$_3$ and 0.1 M NaCl, pH 8.3) to yield a dye/protein ratio of 2:1. The reaction mixture was incubated at room temperature for 1 h. Labeled protein was separated from unreacted dye by gel filtration chromatography on prepacked Sephadex G-25 columns (PD-10, Pharmacia, Uppsala, Sweden) preequilibrated with 20 mM MOPS and 250 mM NaCl, pH 7.8.

Lysozyme was simultaneously labeled with rhodamine and tagged with biotin. The procedure was essentially the same as that described above for labeling of streptavidin with rhodamine succinimidyl ester. However, in addition to the RSE, a biotin−SE derivative, dissolved in

dry DMF, was added to the reaction mixture at a biotin/lysozyme ratio of 8:1. The ability of the biotin-tagged lysozyme to bind streptavidin was confirmed qualitatively. An aliquot of iminobiotin-derivatized agarose (Immunopure Immobilized Iminobiotin, Pierce, Rockford, IL) was incubated with fluorescein-labeled streptavidin, and the gel was pelleted by centrifugation. The yellow color of the fluorescein was localized in the gel, indicating the protein had been bound by the iminobiotin moieties. The supernatant was drawn off, and a solution of rhodamine/biotin-labeled lysozyme was added to the gel. The protein and gel were mixed briefly, and the gel was pelleted by centrifugation. Again, most of the red color of the rhodamine was localized in the gel, indicating the lysozyme was bound to the free biotin pockets of the previously bound streptavidin.

Fluorescence Microscopy. Fluorescence microscopy was performed essentially as described.[21] For polarized fluorescence studies, plastic polarizing sheets (Edmund Scientific C43,781) were placed in the excitation path just before the excitation filter. The excitation polarizers, oriented 90° with respect to each other, were placed in a slider such that the polarizers could be interchanged rapidly. The images were obtained *via* a variable-gain image intensifier (Hamamatsu C2400-68) with a solid-state CCD camera (Hamamatsu C2400-60) and were recorded on a video cassette recorder or digitized directly using a frame grabber (AG-5, Scion Corp., Frederick, MD) on a Macintosh compatible computer (Power 100, Power Computing, Austin, TX). (The AG-5 frame grabber allows multiple frames to be averaged, improving image quality of low-contrast, low-light samples. The images presented are most commonly averages of five consecutive frames.) Images were manipulated using the program NIH Image (developed at the U.S. National Institutes of Health and available on the Internet at http://rsb.info.nih.gov/nih-image/).

(43) Brinkley, M. *Bioconjugate Chem.* **1992**, *3*, 2−13.

JA964099E